

TABLE I. Emulsion characteristics.

Designation	Old type*	New type**
Emulsion thickness	40 $\mu$	24 $\mu$
Emulsion weight	5.4 mg/cm <sup>2</sup>	7.2 mg/cm <sup>2</sup>
Percentage gelatin	56	27
Percentage silver halide	44	73

\* Characteristic of Eastman Emulsion No. 276,296.

\*\* Characteristic of Eastman Emulsion No. 329,489.

emulsion. The photographic density of the images produced by delayed development,  $D_t$ , and of the control developed immediately after the exposure,  $D_0$ , were measured on a recording densitometer. The fractional loss of photographic density as a function of the period of delayed development is exhibited in Fig. 1. The data shows that fading takes place in both emulsions, but is less pronounced in the newer type of high silver halide content.

Since the density is an integration of the blackening produced by the individual alpha-particles, variations in either the length, grain size, or grain spacing of the individual tracks can be anticipated after prolonged delay in their development. Photo-micrographs of the tracks (Fig. 2) show that alterations of this character are produced, the deterioration depending on the emulsion type and the extent of delayed development. It is noteworthy that the tracks are completely obliterated in the emulsions of low silver content if development of the latent image is delayed beyond 5 days, whereas in the improved plates the track is still recognizable after a delay period of 20 days.

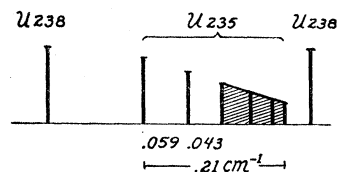
These studies indicate that the abundance of stars in emulsions exposed at high elevations may have been underestimated as a result of the fading of the latent image of the multiple tracks in disintegrations produced during the initial stages of the cosmic-ray exposure. In the new type emulsion the exposure can probably be prolonged for 20 days without appreciable loss in the total track count. Further experiments are in progress on the rate of fading as a function of the energy and the relative flux of the alpha-particles.

<sup>1</sup> H. Yagoda, *Am. Mineralogist* **31**, 87 (1946).<sup>2</sup> M. Blau, *Sitz. Akad. Wien, Math.-Naturw. Klasse, Abt. 2A* **140**, 623 (1931).<sup>3</sup> J. Lauda, *ibid.*, **Abt. 2A** **145**, 707 (1936).<sup>4</sup> G. P. S. Occhialini and C. F. Powell, *Nature* **159**, 186 (1947).

### Hyperfine Structure and the Nuclear Spin of $U^{235}$ \*

O. E. ANDERSON AND H. E. WHITE  
*University of California, Berkeley, California*  
 May 22, 1947

THE hyperfine structure and isotope shift in the arc lines of uranium have been studied using Fabry-Perot etalons with a resolving power of 500,000. The source was a liquid-air cooled hollow cathode tube into which was placed a 50-mg piece of metallic uranium with the isotope 235 considerably enriched. While many of the arc lines in the visible region show isotope shift, only  $\lambda 5915$  and  $\lambda 6926$ , throughout the range of 4000 to 8500A, show resolvable and measurable hyperfine structure.  $\lambda 5027$

FIG. 1. Flag pattern in the hyperfine structure of  $U^{235}$ .

shows a very large isotope shift of  $0.426 \text{ cm}^{-1}$  or  $0.108A$ . Since this line showed no hyperfine splitting of any kind, it was used to check the relative intensities of the two components due to the two isotopes 235 and 238 of the enriched sample.

Using 6-mm etalon spacers, the two components of  $\lambda 5027$  are so sharp and well separated that this line lends itself quite well to relative abundance measurements by either photographic or direct reading photo-voltmeter methods. The photographic method was used in this experiment to compare relative intensities with relative abundance. Agreement to within one percent of the values known from other reliable data is well within the accuracy expected by the photographic method.

Using  $J$ -values supplied to us from other sources,<sup>1</sup> as 6 and 7 for  $\lambda 5915$ , the relative intensities of the components were studied. The flag pattern in the photographs shows three clearly resolved components as indicated in Fig. 1. Knowing the relative abundance of the two isotopes, and hence the relative energies falling into the two isotope patterns, a reasonably good determination of the nuclear spin  $I$  can be made by comparing the 238 sharp component with the first component of the flag pattern. This turned out to be more reliable than a comparison of the relative intensities of the lines within the hyperfine structure pattern or a comparison of their relative intervals.

Assuming the  $J$ -values of 6 and 7, intensity measurements indicate  $I=5/2$ , or  $7/2$ . The over-all width and the relative intensity of the tail of the pattern favor the lower value of  $I=5/2$ .

\* This report is based on work performed under Contract No. W-7405-eng-36 with the Manhattan Project at the Los Alamos Scientific Laboratory of the University of California.  
<sup>1</sup> C. C. Kiess, C. J. Humphreys, and D. D. Laun, *J. Opt. Soc. Am.* **36**, 357 (1946).

### The Concentration of $He^3$ in the Liquid and Vapor Phases of $He^{4*}$

HENRY A. FAIRBANK AND C. T. LANE  
*Sloane Physics Laboratory, Yale University,*  
*New Haven, Connecticut*

AND

L. T. ALDRICH AND ALFRED O. NIER  
*Department of Physics, University of Minnesota,*  
*Minneapolis, Minnesota*  
 May 21, 1947

IT is known<sup>1</sup> that helium contains a stable isotope of mass 3 and that this isotope has an abundance ratio of approximately  $1.3 \times 10^{-6}$  in atmospheric helium and  $1.6 \times 10^{-7}$  in helium derived from natural gas.<sup>2</sup> In order to obtain information on the possibility of separating this isotope with the use of liquid helium, we have studied the

distribution of the isotopes in the liquid and vapor phases as a function of temperature from the normal boiling point down to 2.2°K.

Figure 1 is a schematic drawing of the helium cryostat.

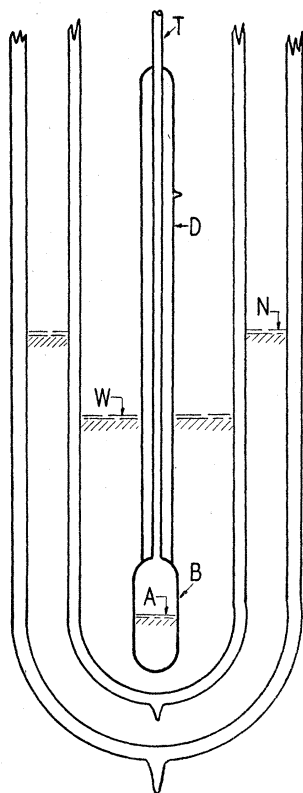


FIG. 1. Schematic drawing of the helium cryostat.

Approximately 2 liters of Air Reduction Company atmospheric helium were condensed into the small Pyrex bulb, *B*, of volume 6 cm<sup>3</sup>. The gas is introduced through a glass capillary, *T*, approximately 1.5 mm in diameter. Surrounding *T* is a vacuum jacket, *D*, serving as an insulating Dewar to prevent solidification of impurities which might block the capillary. A mercury Toepler pump is employed to displace the helium into bulb *B* from the storage flask.

TABLE I. Concentration of He<sup>3</sup> relative to He<sup>4</sup>.

Sample	He <sup>3</sup> /He <sup>4</sup> in reference samples	He <sup>3</sup> /He <sup>4</sup> in vapor ( <i>C<sub>v</sub></i> )	He <sup>3</sup> /He <sup>4</sup> in liquid ( <i>C<sub>L</sub></i> )	$\frac{C_v}{C_L}$	<i>T</i> (°K)
0	1.2 × 10 <sup>-6</sup>				297
1		1.9 × 10 <sup>-6</sup>	1.33 × 10 <sup>-6</sup>	1.4	4.21
2		2.1	1.33	1.6	3.90
3		2.3	1.33	1.7	3.60
4		3.3	1.28	2.6	3.30
5		4.0	1.27	3.1	3.00
6		5.6	1.28	4.4	2.69
7		6.5	1.29	5.0	2.40
8		8.0	1.27	6.3	2.20
9	1.3				297
10	1.3				297

Surrounding bulb *B* is a bath of liquefied well helium, *W*, the temperature of which may be controlled by reducing its vapor pressure by means of a vacuum pump. A second bath of liquid nitrogen, *N* serves as a radiation shield. By means of slits in the Dewars the bulb *B* is visible at all times. Approximately 3 cm<sup>3</sup> of liquid atmospheric helium was condensed in the bulb, and a differential manometer was employed to assure that the temperatures inside and outside the bulb were equal. Samples of the helium vapor from *B* were collected in break-seal tubes at each temperature listed in Table I. The liquid and vapor in *B* were kept at a constant temperature for 30 minutes before each sample was withdrawn. Sample 0 was taken from the original supply of atmospheric helium and sample 9 from the helium gas recovered at the end of the experiment when the liquid helium in bulb *B* had completely evaporated.

The isotope analyses were made with the same instrument mentioned in reference 2. Sample 10 was from another batch of atmospheric helium also supplied by the Air Reduction Company and happens to be one used as a comparison standard for current work on the mass spectrometer. All analyses except that of sample 0 were done the same day. One would expect samples 0 and 10 to be identical, whereas sample 9 should show a slightly smaller He<sup>3</sup> concentration because of preferential depletion of He<sup>3</sup> caused by successive sampling. While samples 0 and 10 agree within the error to be expected in measurements of this sort, it seems preferable to use sample 9 in our computations. In Table I are listed also the He<sup>3</sup>/He<sup>4</sup> concentrations in the vapor (*C<sub>v</sub>*) and in the liquid (*C<sub>L</sub>*). *C<sub>L</sub>* is computed from *C<sub>v</sub>* and the mass and composition balance equations making use of the Leiden data for vapor and liquid densities.<sup>3</sup> Correction has been applied for the successive depletion in He<sup>3</sup> because of the withdrawal of the samples. The average sample was roughly 10 cm<sup>3</sup> (STP).

Figure 2 is a plot of the relative concentrations in the

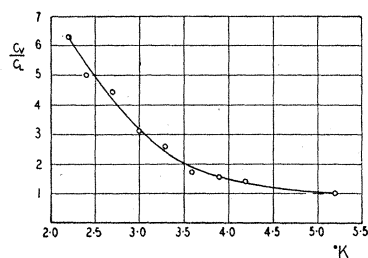


FIG. 2. The relative He<sup>3</sup>/He<sup>4</sup> concentration in the vapor to that in the liquid as a function of temperature.

vapor and liquid as a function of temperature. Since 5.2°K is the critical temperature of helium, this ratio must be unity at this temperature.

No attempt has been made to interpret these data theoretically, but it is clear that if pure He<sup>3</sup> exists as a liquid it must have a lower boiling point than He<sup>4</sup>. Inasmuch as the liquid contains a sizable proportion of the He<sup>3</sup> isotope, it appears possible to check whether this isotope participates in the superflow properties of He<sup>4</sup> by

allowing the liquid to leak out of a closed container through a superleak and measuring the concentration of the residual gas.

\* The work at Yale University was assisted by the Office of Naval Research under Contract N6ori-44 and that at the University of Minnesota by grants from the Research Corporation and the Graduate School.

<sup>1</sup> L. W. Alvarez and R. Cornog, *Phys. Rev.* **56**, 613 (1939); **56**, 379 (1939).

<sup>2</sup> L. T. Aldrich and A. O. Nier, *Phys. Rev.* **70**, 983 (1946). At the time this work was done we did not feel that the accuracy of the measurements justified a correction for the difference in pumping speeds of He<sup>3</sup> and He<sup>4</sup> in the mass spectrometer pump lead. We now feel that the accuracy justifies this correction. Hence He<sup>3</sup> abundances previously given should be multiplied by (4/3)<sup>3</sup>.

<sup>3</sup> E. Mathias, C. A. Crommelin, H. K. Onnes, and J. C. Swallow, *Leiden Comm.* 172b (1925).

### Conductivity Pulses Induced in Diamond by Alpha-Particles

D. E. WOOLDRIDGE,\* A. J. AHEARN, AND J. A. BURTON  
*Bell Telephone Laboratories, Murray Hill, New Jersey*  
May 21, 1947

THE modern theory of the solid state predicts that when alpha-particles bombard an insulator, the electrons freed by ionization will be raised to the conduction band. Under the influence of an applied electric field, these electrons, and the positive holes in the normally filled band, should move just as in the case of photo-conductivity. With a sufficiently high electric field across an insulator crystal which is relatively free of electron traps, it should be possible under favorable conditions to detect the movement of these charges and thus observe conductivity pulses.

With an amplifier and cathode-ray oscilloscope we have observed such pulses, produced by individual alpha-particles from radium, in diamond crystals at room temperature. The number of ions produced in diamond is of the same order as the number of ions produced by alpha-particles in an air ionization chamber. These conductivity pulses have been observed with two markedly different electrode arrangements on the diamond. One system consists of a pair of metal electrodes deposited by evaporation on the surface of the diamond, these electrodes being separated by a gap of 0.003 cm. Here the conductivity pulses consist of charges which travel across the top surface layers of the gap on the diamond. Good pulses were obtained with 5 volts applied across this gap. The second arrangement consists of evaporated electrodes on opposite sides of a diamond chip of about 0.5-mm thickness. Here the conductivity pulses consist of charges which travel from one surface toward the other surface of the diamond. Good pulses were obtained with 100 volts across such a diamond. In general, applied fields as low as 2000 volts per cm may be sufficient to approach saturation.

With each of the above electrode systems, pulses of comparable size are obtained with either direction of the applied field. When the applied field is reduced to zero, pulses are observed but for a short time only. These "space-charge" pulses are opposite in direction to those that occur when the voltage is applied, i.e., the diamond becomes polarized.

Our diamond specimens consist chiefly of "saw cuts," i.e., small chips sawed from a natural diamond in eliminat-

ing flaws, etc. Most of the diamonds which we have tested show this alpha-particle bombardment-induced conductivity. However, no conductivity pulses were observed in some diamonds even though saturation in photo-conductivity is approached at the applied fields used in the alpha-particle bombardment tests.

The electrodes apparently need to be in intimate contact with the diamond surface. Electrodes of gold, aluminum, or platinum formed by evaporation are satisfactory.

Van Heerden<sup>1</sup> has observed conductivity pulses induced by alpha-particle bombardment of silver chloride crystals at liquid nitrogen temperature, but he found none in the single diamond that he tried.

This phenomenon of bombardment-induced conductivity in diamond immediately suggests its use as a solid counter for nuclear physics experiments, particularly since it operates at room temperature. Its small size, high density, low operating voltage, and the possibility of rapid counting rate may give the diamond solid counter certain advantages over the conventional gas type counter.

\* Now at Hughes Aircraft Company, Culver City, California.  
<sup>1</sup> P. J. Van Heerden, Thesis (Utrecht, 1945).

### Structure of the Quadrielectron\*

AADNE ORE  
*Sloane Physics Laboratory, Yale University,*  
*New Haven, Connecticut*  
May 15, 1947

A PREVIOUS calculation led to the approximate value 0.11 ev for the binding energy of a system of two electrons and two positrons against dissociation into two free bielelectrons.<sup>1</sup> The variational function leading to this result is the generalized "atomic" function

$$\psi_{\beta} = \frac{1}{2} \left\{ \exp -\frac{1}{2} [(1+\beta)(r_{1a}+r_{2b}) + (1-\beta)(r_{1b}+r_{2a})] \right. \\ \left. + \exp -\frac{1}{2} [(1-\beta)(r_{1a}+r_{2b}) + (1+\beta)(r_{1b}+r_{2a})] \right\}$$

where 1 and 2 refer to the electrons and *a* and *b* to the positrons.

This numerical result represented a considerable improvement as compared with the energy values resulting from earlier calculations, but it gave little information regarding the true value of the energy. For this reason an attempt has been made to determine the energy of the quadrielectron with greater accuracy.

The function,  $\psi_{\beta}$ , is related to the function used by S. C. Wang in the problem of the energy of the normal hydrogen molecule. A calculation has now been performed which is similar rather to Weinbaum's treatment of the hydrogen molecule by means of a linear combination of "atomic" and "ionic" functions,<sup>2</sup> which led to a considerable improvement in the energy value as compared to Wang's result.

For this purpose the following function has been used:  $\Psi = \psi_{\beta} + c\psi_{\alpha}$ , where the "ionic" function,  $\psi_{\alpha}$ , is defined by

$$2\psi_{\alpha} = \exp -\frac{1}{2} [(1+\alpha)(r_{1a}+r_{2a}) + (1-\alpha)(r_{1b}+r_{2b})] \\ + \exp -\frac{1}{2} [(1-\alpha)(r_{1a}+r_{2a}) + (1+\alpha)(r_{1b}+r_{2b})] \\ + \exp -\frac{1}{2} [(1+\alpha)(r_{1a}+r_{1b}) + (1-\alpha)(r_{2a}+r_{2b})] \\ + \exp -\frac{1}{2} [(1-\alpha)(r_{1a}+r_{1b}) + (1+\alpha)(r_{2a}+r_{2b})].$$

Since  $\Psi$  does not contain the distances between particles